CHAPTER 8 STUDIES OF ACICULAR FERRITE BY THIN FOIL TEM

8.1 Acicular ferrite morphology in experimental alloys

The optical micrographs in figure 7.29 for the alloys after rapid cooling at a rate of 47 $^{o}Cs^{-1}$, show a typical acicular ferrite microstructure, also according to the literature[4,65,131,134]. No researcher in any of these references reported the presence of any polygonal ferrite in an acicular ferrite microstructure, however, even though their optical microstructures appear very similar to those in this study (figure 7.29). Polygonal ferrite is of a "polygonal" shape with a lightly etched colour of "white" in its microstructures under an optical microscope after being etched in a 2% Nital solution. But acicular ferrite also appears as a white plus grey or striated phase in microstructures under some etching conditions. Previous researchers[4,65,131,134] have accepted that optical micrographs like figure 7.29-(b) to (f), consist of only acicular ferrite. As mentioned in section 7.9.3 above, however, the TEM observations on carbon extraction replicas in this study with Au-Pd shadowing, as represented by the microstructures of alloys #1 to #5, are obviously a mixture of polygonal ferrite plus acicular ferrite. A final conclusion based only on the somewhat ill-defined optical microscopy but more clearly confirmed by the observations on shadowed extraction replicas is, of course, not satisfactory in itself and TEM observations on thin foils were done to confirm more details of this apparent anomaly with conclusions reached by other researchers in these microstructures.

Furthermore, it should be recognised that the latest understanding on the nature and origin of acicular ferrite in wrought line pipe steels, is that it may not necessarily be a "unique singular phase" (for instance, the "chaotic morphology" found in welds) but that acicular ferrite should rather be understood as a *collective term* describing a microstructure containing possibly more than one type of ferrite phase, all of which have nucleated intragranularly. It will be seen that this broader concept of what acicular ferrite in line pipe steels really is, is supported by the results of this work here below where two different morphologies of intragranularly nucleated ferrite laths were found, i.e. a "chaotic" arrangement (as in the "classical" acicular ferrite in welds) as well as an arrangement of "parallel laths" somewhat similar to classical bainite except for its nucleation intragranularly.

8.1.1 Acicular ferrite and polygonal ferrite in alloy #6 (Mo-free)

(i) Acicular ferrite and polygonal ferrite

Figure 8.1 below represents the thin foil TEM micrographs of the Mo-free alloy #6 after a rapid cooling rate of 39 $°Cs^{-1}$ after the hot rolling process. A "polygonal" shaped phase could be observed in figure 8.1-(a) (marked with "PF"). According to its shape it appears to be polygonal ferrite with a size of approximately 5 μm in diameter. Many laths in the structure (marked "lath" in the figure) were found beside the polygonal ferrite. The shape of the "PF" is quite different from that of the laths in this figure with the latter more elongated in their shape. This is consistent with the observation from figure 7.34 and discussed in the introduction in section 8.1 above.

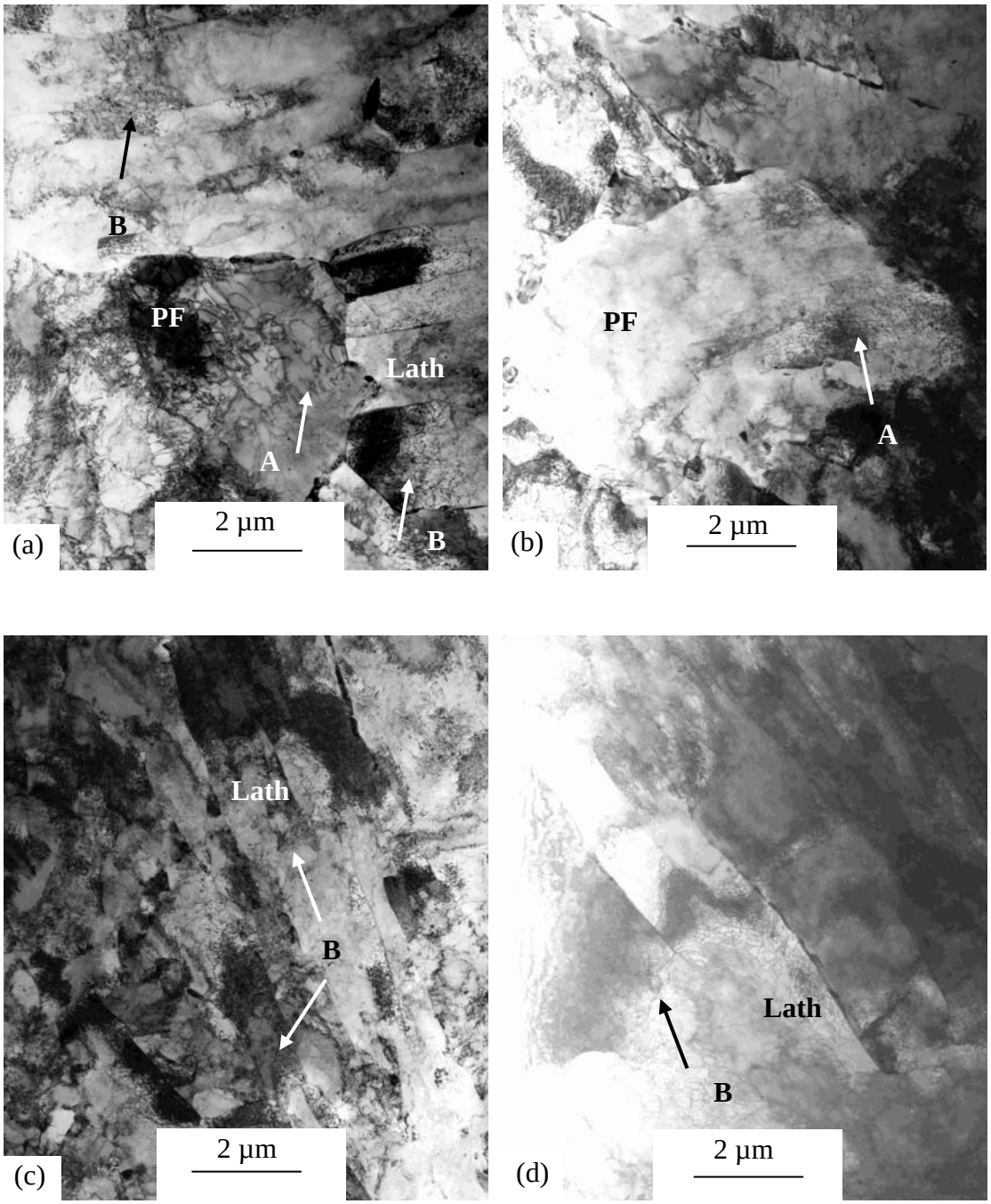

Figure 8.1 Thin foil TEM micrographs of alloy #6 (Mo-free) after a rapid cooling rate of 39 °Cs^{-1} after hot rolling, (a) polygonal ferrite + laths, (b) polygonal ferrite with dislocations and, (c),(d) laths with dislocations. PF-polygonal ferrite, AF-acicular ferrite, A and B-dislocations in polygonal ferrite and an acicular ferrite , respectively.

Another polygonal ferrite grain with size of about 5.8 µm in figure 8.1-(b) is also evident. No cementite was found within the laths or on inter-lath boundaries. This means that the laths are in all likelihood part of acicular ferrite instead of bainite where cementite would be present within the laths in lower bainite and on inter-lath

position in upper bainite[97]. The carbon rejected from the acicular ferrite laths may possibly be in martensite/austenite islands enriched in carbon as no cementite was found in the thin foils. A further study of the martensite/austenite islands in these steels probably needs further thin foil TEM work to confirm it.

According to the CCT diagrams of alloy #6 (see figure 7.22), the polygonal ferrite probably forms during cooling first at higher temperature and the acicular ferrite later. The acicular ferrite is, therefore, mixed in between the polygonal ferrite. Polygonal ferrite can not be fully distinguished from an acicular ferrite on optical micrographs alone such as in figure 7.29-(f), but combining optical and TEM observations of alloy #6 in figure 7.29-(f), it appears that the laths (see figure 8.1) are most likely from an acicular ferrite and not bainite because of the less visible grain boundaries[131,135] and no cementite within or between the laths was observed after deep etching. A further study on this lath structure is made below. It is, therefore, concluded that the microstructure of alloy #6 is most probably a mixture of acicular ferrite and polygonal ferrite.

(ii) Dislocations within the polygonal ferrite

Dislocations were also observed within the polygonal ferrite (see figures 8.1 and 8.2) in these line pipe steels. This is somewhat different, for instance, from polygonal ferrite found in plain low carbon steels where generally dislocation-free polygonal ferrite is usually found. This has led to some researchers even referring to “quasi-polygonal ferrite” in wrought low alloy steels. The reason for this difference caused by alloying elements, requires further investigation but may be associated with solute drag of dislocations by alloying elements, thereby hindering their movement and recovery whereas this is largely absent in plain low carbon steels.

Figure 8.2 showed that there were dislocations apparently being emitted (marked with “M”) from the area close to the moving interface of the PF. There were also more dislocations near this moving interface than within the central regions of the PF (marked with “L”). These dislocations were possibly generated during the formation of polygonal ferrite within the austenite. Firstly, according to the CCT diagram of alloy #6 (see figure 7.26), the polygonal ferrite was formed in a higher temperature

range than that of acicular ferrite. Secondly, there was a volume expansion of about 3.6% (calculated for a 0.06% C steel) during polygonal ferrite formation from austenite as the lattice changed from face-centered cubic (austenite) to body-centered cubic (polygonal ferrite). This will lead to the transformed polygonal ferrite that was surrounded by the parent austenite, to undergo a compression strain of about 1.2% from the austenite. Because of the relatively high temperatures at this stage and hence a low flow stress in the ferrite, this linear strain will probably be a plastic one, thereby creating interface dislocations in the ferrite near the interface as it advances into the austenite.

In addition, however, a second volume expansion again of about 3.6% occurs at a slightly lower temperature as the surrounding austenite now transforms to the bcc acicular ferrite, with the less dense acicular ferrite now creating a further strain field[74,76] on the already formed polygonal ferrite. Such a strain field from acicular ferrite formation leads to a high dislocation content in the acicular ferrite from the displacive transformation but also from some plastic strain within the adjacent austenite[75] or the already existing polygonal ferrite due to the lattice volume change.

Both of these volume expansion processes will result in strain or deformation to be concentrated within the outer edges of the polygonal ferrite rather than in the centre. Therefore, there were more dislocations found in the edge region (marked by “M”) than in the centre region of the polygonal ferrite (marked by “L”). Figures 8.1-(a) and 8.2 show the acicular ferrite that was situated around the polygonal ferrite.

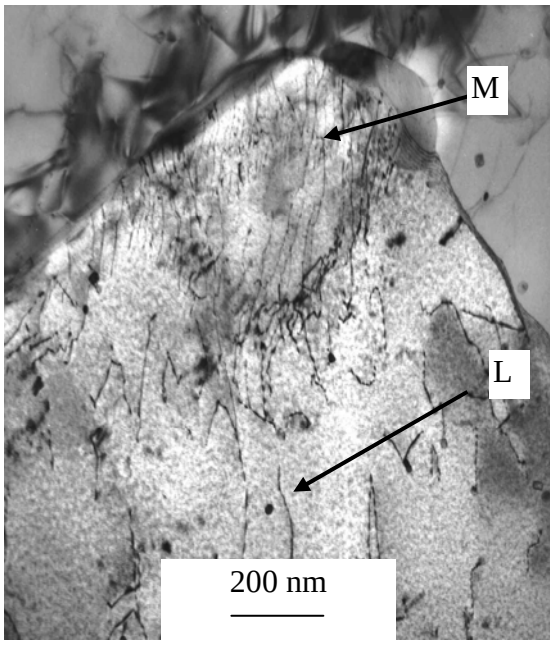

Figure 8.2 Dislocations within the polygonal ferrite in thin foil of the Mo-free alloy #6. The area M shows a high density of dislocations possibly being emitted from the moving PF interface while the central regions L of the PF have less dislocations.

8.1.2 Acicular ferrite and polygonal ferrite in alloy #1

Alloy #6 was the current Mittal Steel's line pipe steel, i.e. V-Nb-Ti micro-alloyed. The main difference between the experimental alloy #1 and the reference alloy #6 was in the niobium and carbon contents. The niobium content in alloy #1 had been increased to 0.055%wt Nb and the carbon content lowered to 0.05%wt C in order to obtain a higher degree of dispersion hardening in the ferrite. TEM thin foil micrographs of polygonal ferrite in this study are shown in figure 8.3, in which a high density of dislocations was also observed with a high magnification.

Figure 8.4 represents an interwoven lath structure from alloy #1 and a high density of dislocations was found within laths B and C. Lath A is not parallel to laths B and C. This is a typical interwoven structure of acicular ferrite, also reported in the literature[4,65,131,134]. Another interwoven lath structure with PF present in this alloy #1, is also shown in figure 8.5. Consequently, it is confirmed that the microstructures of alloy #1 with rapid cooling after hot rolling, also consists of a mixture of an acicular ferrite plus polygonal ferrite.

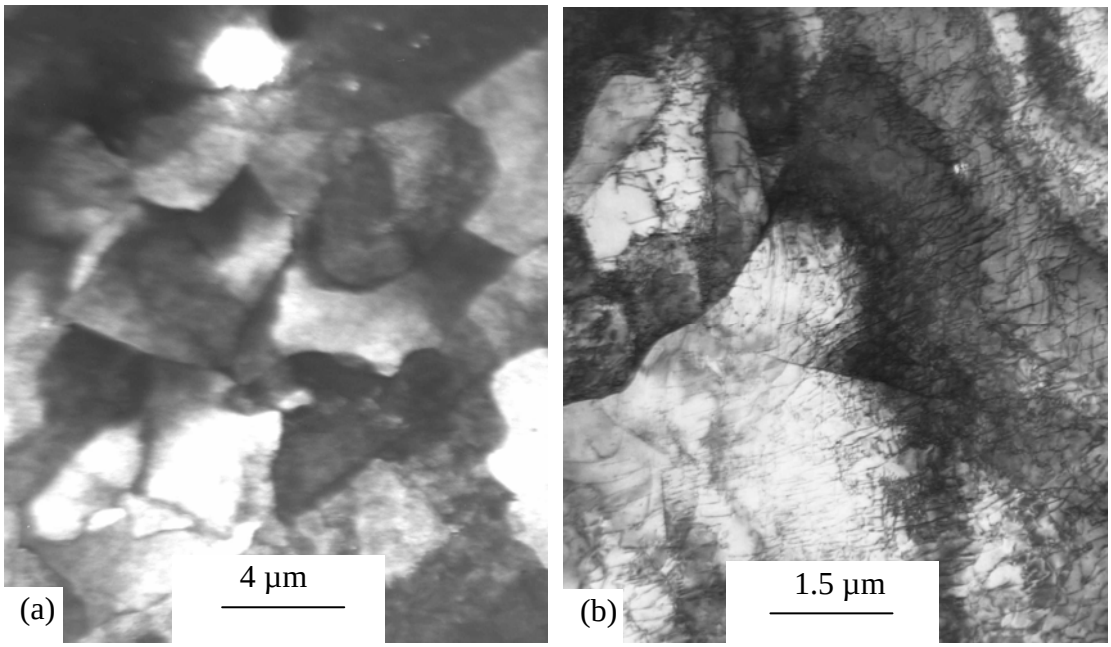

Figure 8.3 Polygonal ferrite in a TEM thin foil micrograph from the experimental alloy #1 after a rapid cooling rate of 47 $^{o}Cs^{-1}$ after the hot rolling process.

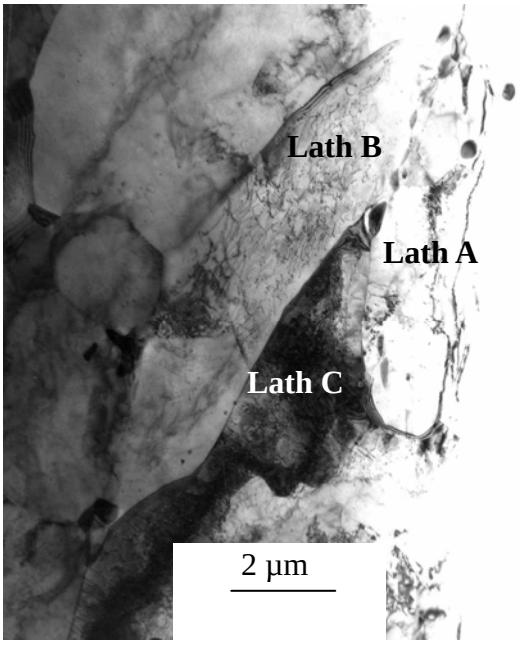

Figure 8.4 TEM thin foil micrograph with laths from alloy #1 after a rapid cooling rate of 47 $^{o}Cs^{-1}$ after the hot rolling process.

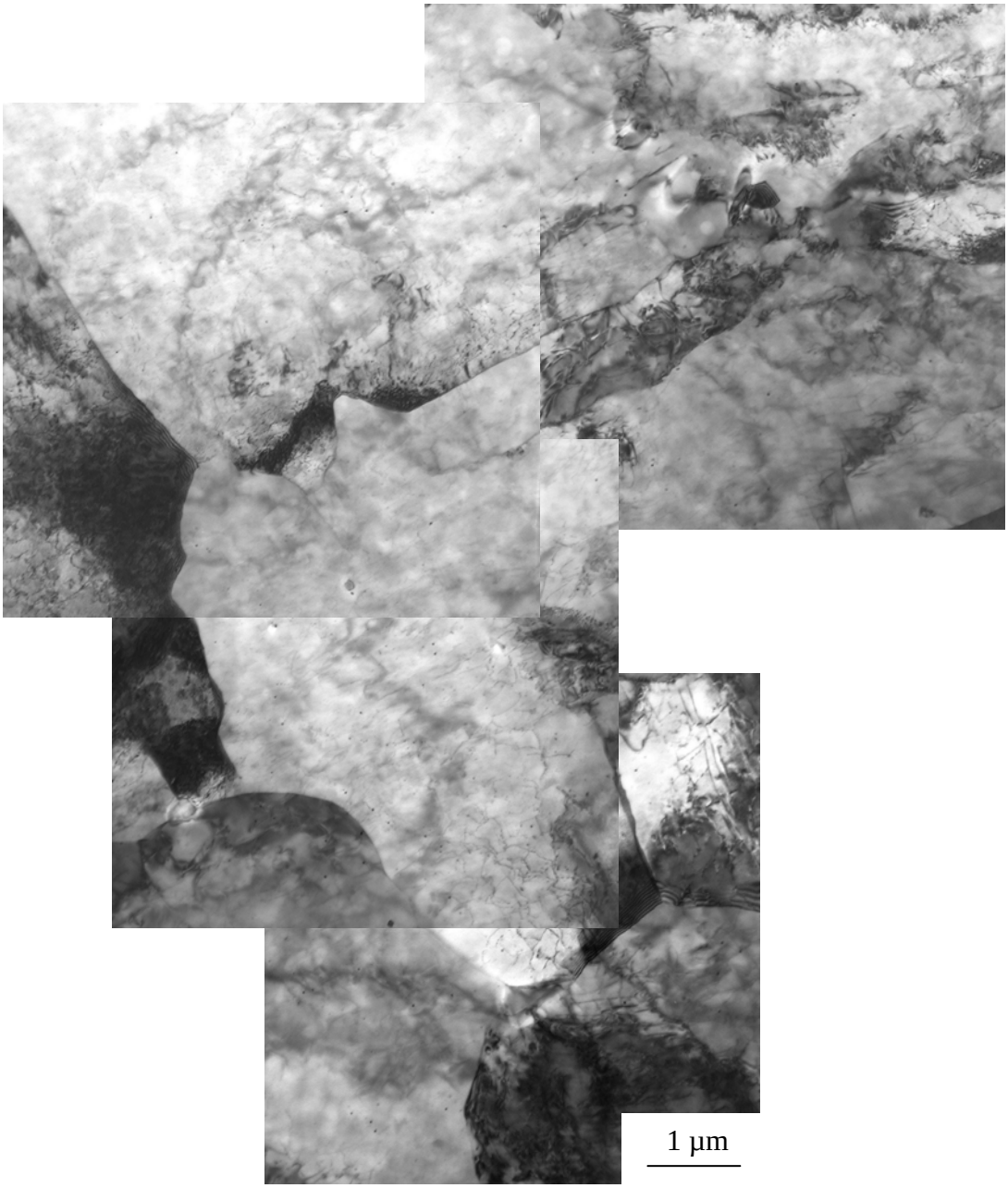

Figure 8.5 TEM thin foil micrograph of the lath plus PF structure in alloy #1 after a rapid cooling rate of 47 $^{o}Cs^{-1}$ after the hot rolling process.

8.1.3 Acicular ferrite in alloys #2 to #5

The lath structures of alloy #2 with an 0.09% Mo + 0.05% Nb addition, are shown in figures 8.6 and 8.7 from TEM thin foils after a rapid cooling rate of 47 $^{o}Cs^{-1}$ after the hot rolling. Parallel laths were found in figure 8.7.

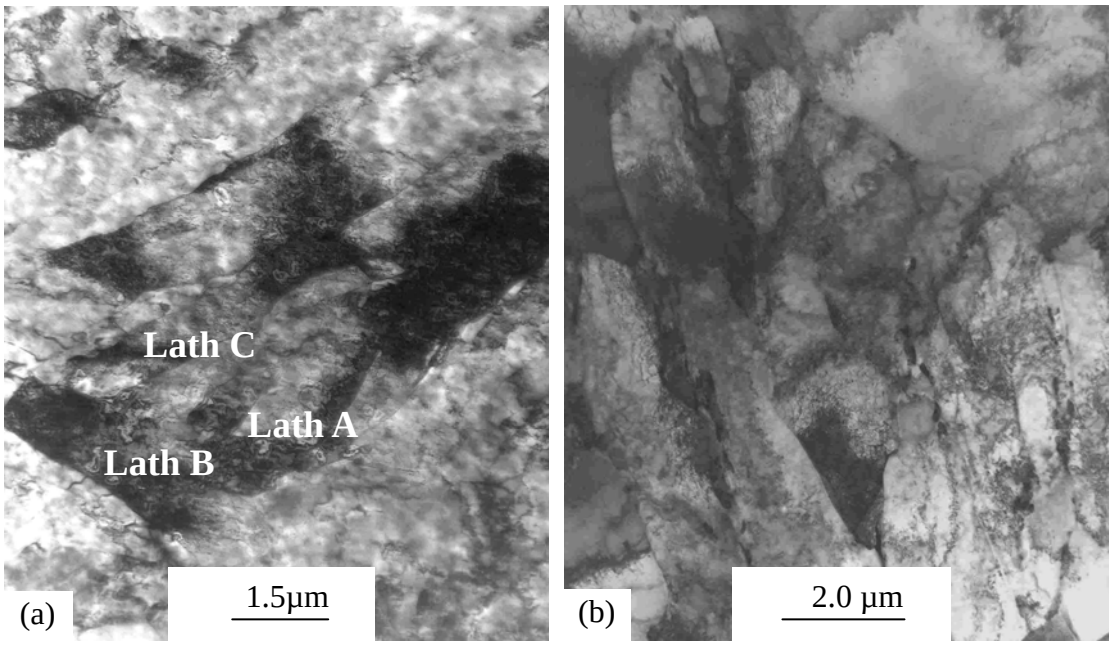

Figure 8.6 Thin foil TEM micrographs of the lath structure in alloy #2 after a rapid cooling rate of 47 $^{o}Cs^{-1}$ after the rolling process.

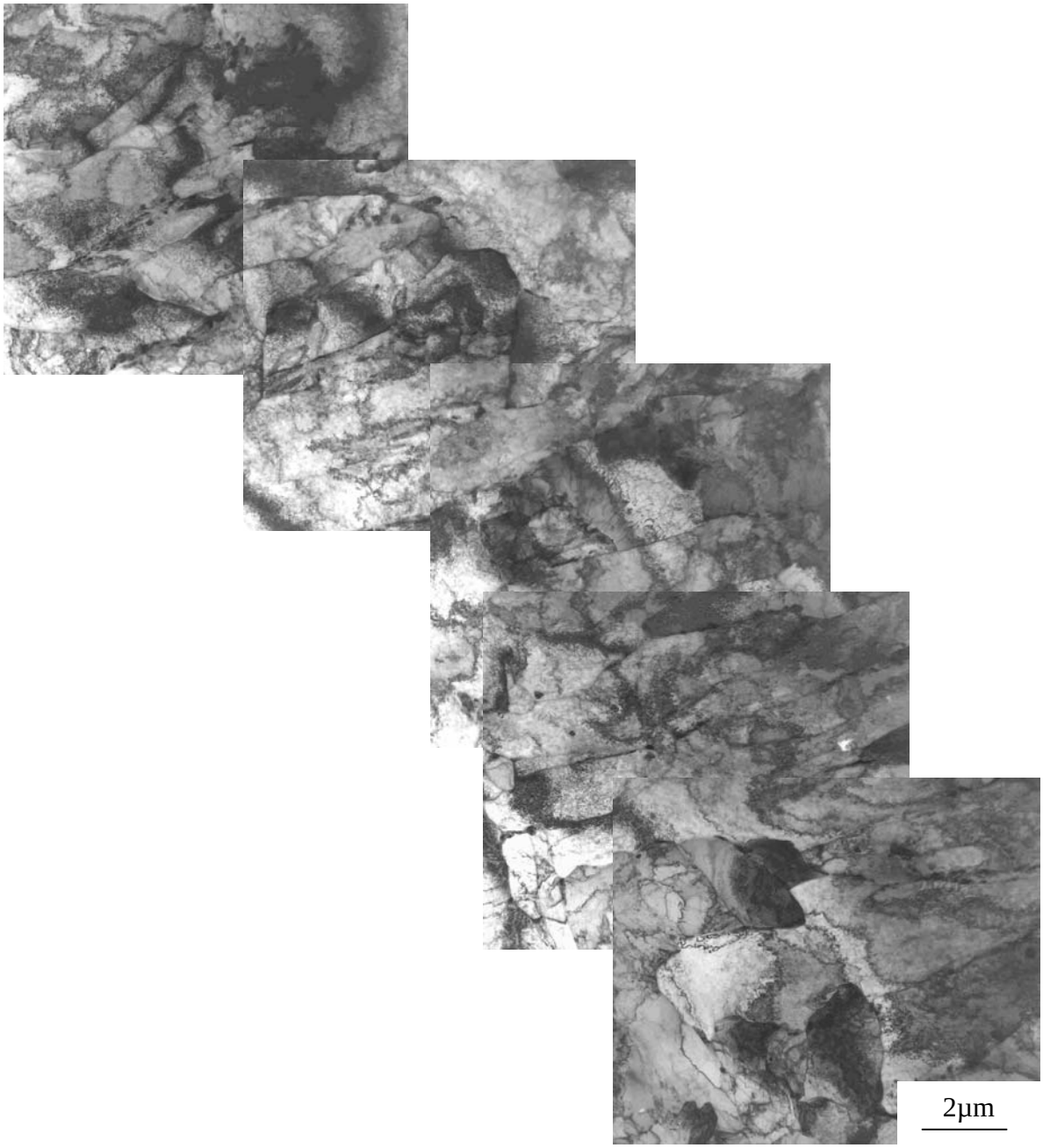

Figure 8.7 Thin foil TEM composite micrographs of parallel laths of an acicular ferrite in alloy #2 after a rapid cooling rate of 47 $^{o}Cs^{-1}$ after the hot rolling process.

Figure 8.8 shows the polygonal ferrite (plus a few isolated laths) found in alloy #3 after a rapid cooling rate of 47 $^{o}Cs^{-1}$ after the hot rolling process. Some dislocations can be found within the polygonal ferrite as well although of a lesser density than in the AF laths. The micrographs with a parallel lath structure of alloy #3 are shown in figure 8.9.

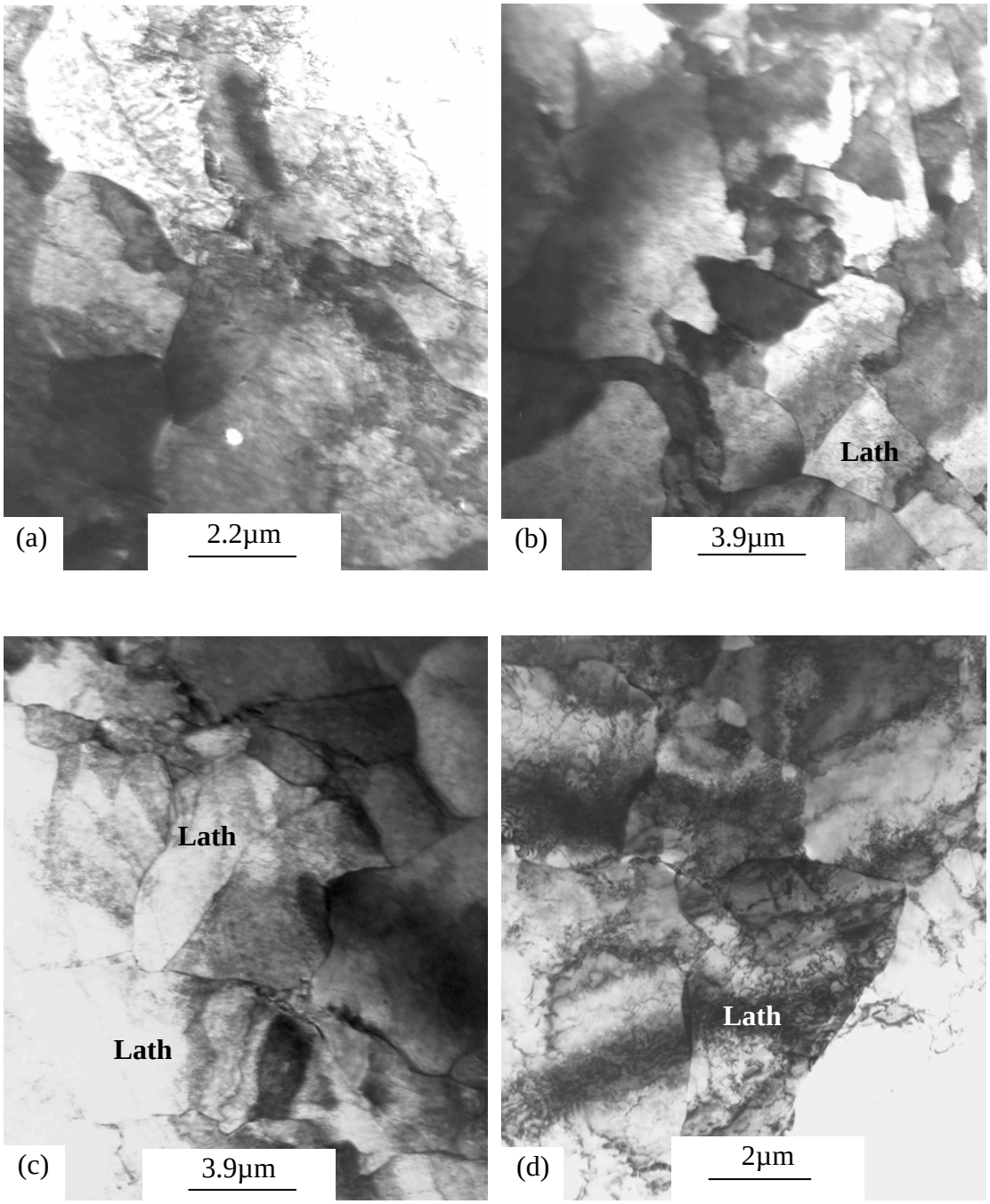

Figure 8.8 Polygonal ferrite (with a few isolated laths) in alloy #3 with a rapid cooling rate of 47 $^{o}Cs^{-1}$ after the hot rolling process.

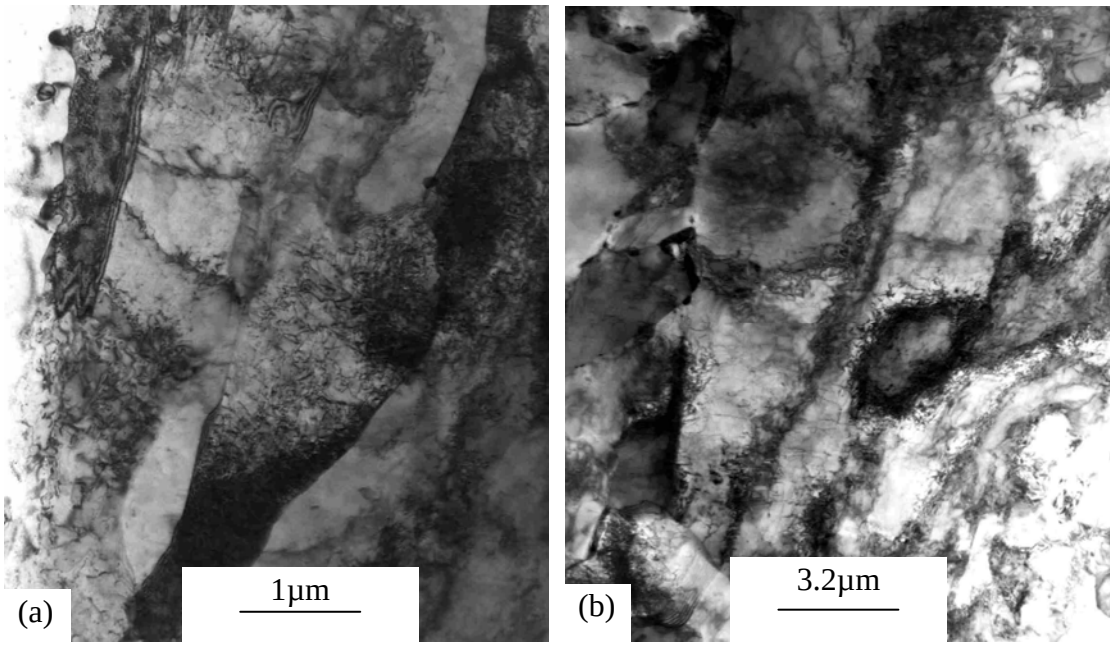

Figure 8.9 The parallel lath morphology in alloy #3 after a rapid cooling rate of 47 $^{o}Cs^{-1}$ after the hot rolling process.

Figure 8.10 shows a composite micrograph of a mixed polygonal ferrite and an acicular ferrite microstructure in alloy #3. Polygonal ferrite is marked with PF in the figure. The interwoven laths are clearly seen, where lath A is crossed by laths B and C.

Figure 8.11 represents the lath structure in alloy #4. Polygonal ferrite with dislocations, can also be found in alloy #5 (with 0.22% Mo) after a rapid cooling rate of 47 $^{o}Cs^{-1}$ (figure 8.12-(a)). An interwoven lath structure of an acicular ferrite in alloy #5 can also be observed in figures 8.12-(b) and (c). It is, therefore, confirmed that the microstructure of alloy #5 (with 0.22%Mo) is also one of polygonal ferrite plus acicular ferrite.

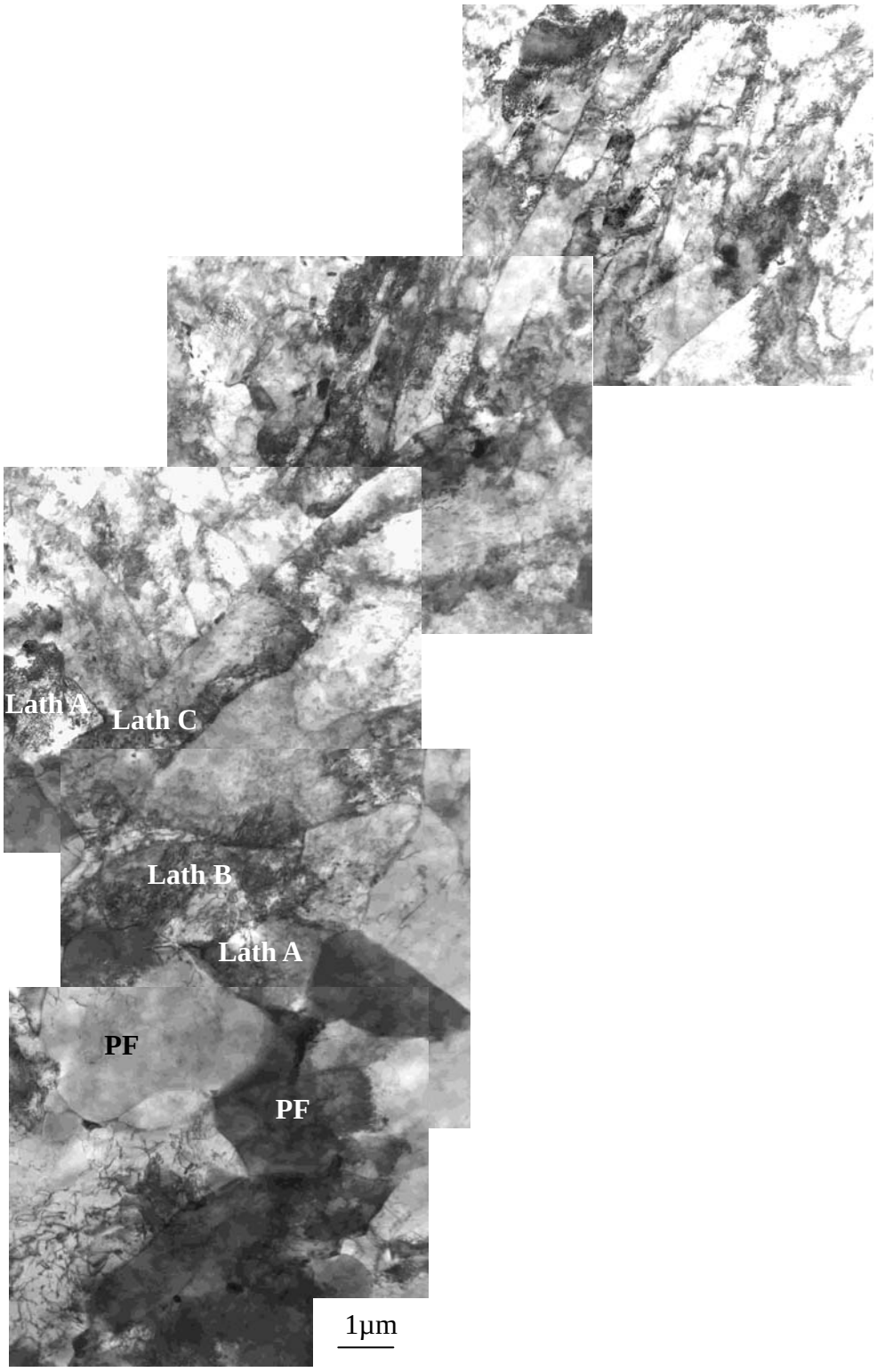

Figure 8.10 Thin foil TEM micrographs of a mixture of polygonal ferrite and an acicular ferrite in alloy #3 after a rapid cooling rate of 47 $^{o}Cs^{-1}$ after the hot rolling process.

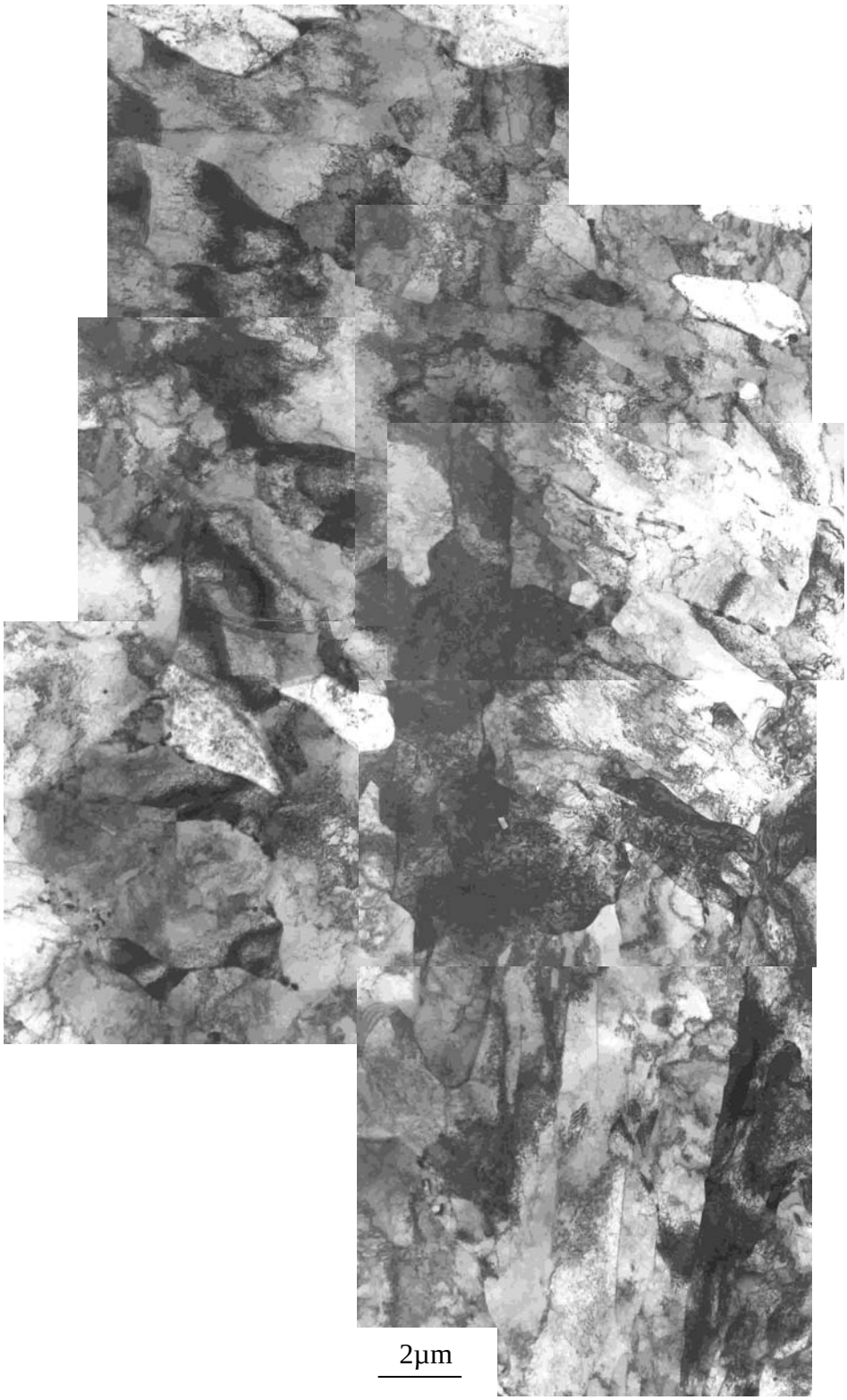

Figure 8.11 Thin foil TEM composite micrographs of the acicular ferrite in alloy #4 after a rapid cooling rate of 47 $^{o}Cs^{-1}$ after the hot rolling process.

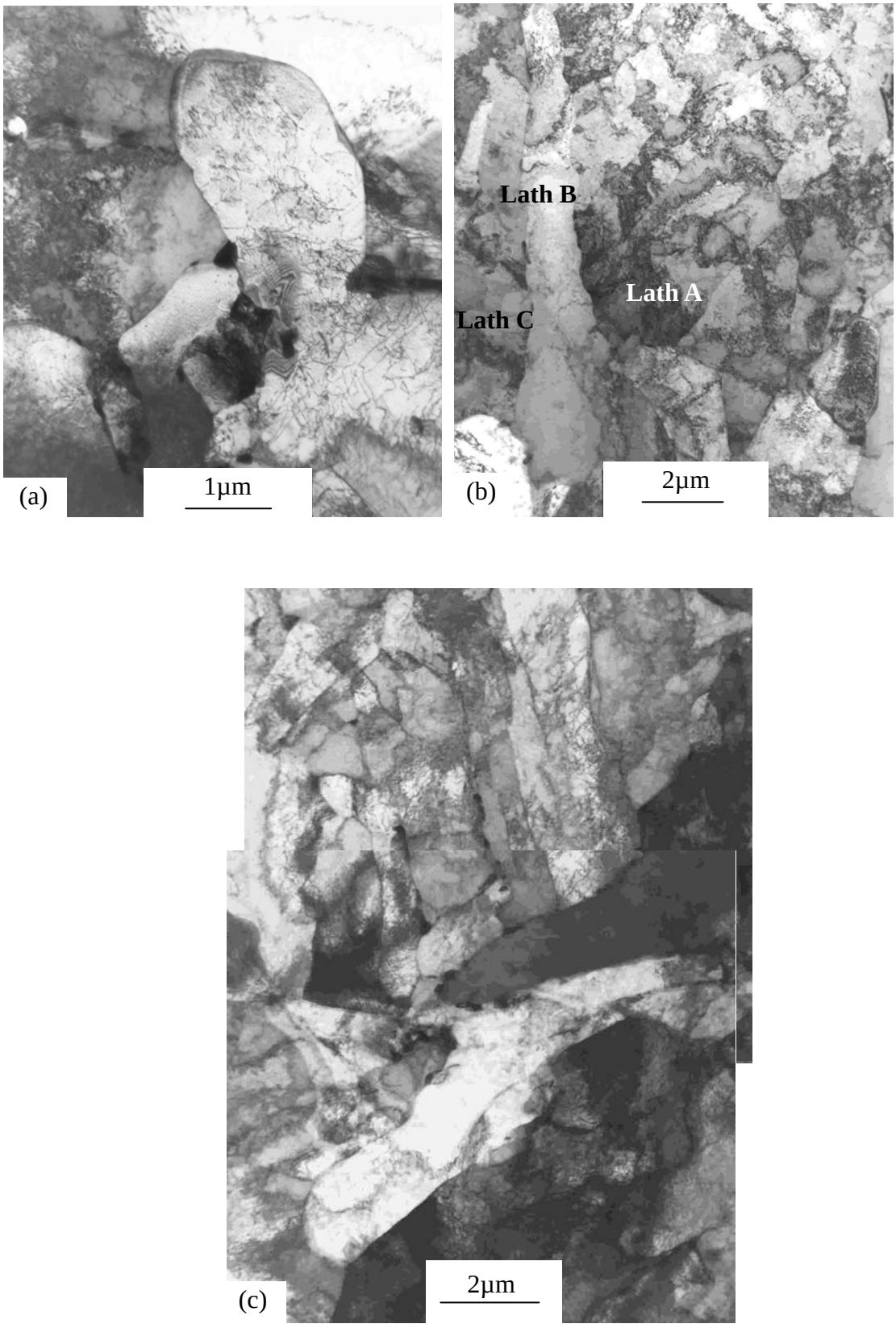

Figure 8.12 Thin foil TEM micrographs from alloy #5 with 0.22% Mo (a) polygonal ferrite, (b) and (c) acicular ferrite with interwoven laths.

Conclusions

Summarising these thin foils results shown above, the following conclusions can be drawn:

- All experimental alloys cooled at a rapid cooling rate of 47 $^{o}Cs^{-1}$ after hot rolling, had a mixed microstructure of polygonal ferrite and an acicular ferrite, as confirmed by thin foil TEM micrographs.
- This confirmed the tentative observation made from the optical micrographs in figure 7.28 that the structure did not appear to be a 100% acicular ferrite but that it rather consisted of a mixture of polygonal ferrite and an acicular ferrite.
- There were no visible etched boundaries between polygonal ferrite and the acicular ferrite microstructure on the optical micrographs. Accordingly, optical micrographs such as in figure 7.29, can not decisively prove by themselves whether there is any polygonal ferrite in a largely acicular ferrite microstructure, as is apparently sometimes inadvertently done in the literature. It can only be confirmed by TEM work on thin foils and shadowed carbon replicas.
- Acicular ferrite has an interwoven lath structure with a high density of dislocations but contained no cementite, neither in the interlath positions or within the laths.
- Polygonal ferrite has a significantly lower dislocation content than the acicular ferrite but some apparent interface emission of dislocations in regions near to the interface into the polygonal ferrite has been observed.